Dual Origin of the Epithelium of the Mammalian Middle Ear

Hannah Thompson and Abigail S. Tucker

Science **339**, 1453 (2013);
DOI: 10.1126/science.1232862

essentially only in human species, it is likely to have evolved to persist in the human population, with a sufficient number of individuals developing pathology to assure transmission by aerosol and survival of the pathogen, the remainder containing the pathogen by protective host immune responses. Therapeutic interventions to block IFN-β–induced pathologic responses as well as enhance in IFN-γ responses may be an effective strategy to alter the balance to favor protection in mycobacterial and other infections.

References and Notes

1. M. Fabri *et al.*, *Sci. Transl. Med.* **3**, 104ra102 (2011).
2. R. M. O'Connell *et al.*, *J. Exp. Med.* **200**, 437 (2004).
3. M. P. Berry *et al.*, *Nature* **466**, 973 (2010).
4. M. Yamamura *et al.*, *Science* **254**, 277 (1991).
5. M. Yamamura *et al.*, *J. Immunol.* **149**, 1470 (1992).
6. S. J. Waddell *et al.*, *PLoS ONE* **5**, e9753 (2010).
7. S. A. Samarajiwa, S. Forster, K. Auchettl, P. J. Hertzog, *Nucleic Acids Res.* **37**, D852 (2009).
8. T. R. Golub *et al.*, *Science* **286**, 531 (1999).
9. S. S. Iyer, A. A. Ghaffari, G. Cheng, *J. Immunol.* **185**, 6599 (2010).
10. M. Rayamajhi, J. Humann, K. Penheiter, K. Andreasen, L. L. Lenz, *J. Exp. Med.* **207**, 327 (2010).
11. P. T. Liu *et al.*, *Science* **311**, 1770 (2006); 10.1126/science.1123933.
12. J. Maertzdorf *et al.*, *Proc. Natl. Acad. Sci. U.S.A.* **109**, 7853 (2012).
13. C. L. Cooper *et al.*, *J. Exp. Med.* **169**, 1565 (1989).
14. D. Montoya *et al.*, *Cell Host Microbe* **6**, 343 (2009).
15. P. T. Liu *et al.*, *Nat. Med.* **18**, 267 (2012).
16. P. T. Liu *et al.*, *PLoS ONE* **4**, e5810 (2009).
17. S. R. Krutzik *et al.*, *J. Immunol.* **181**, 7115 (2008).
18. J. S. Adams, M. A. Gacad, *J. Exp. Med.* **161**, 755 (1985).
19. K. Edfeldt *et al.*, *Proc. Natl. Acad. Sci. U.S.A.* **107**, 22593 (2010).
20. P. Salgame *et al.*, *Science* **254**, 279 (1991).
21. A. N. Martinez *et al.*, *J. Clin. Microbiol.* **47**, 2124 (2009).
22. G. Guarda *et al.*, *Immunity* **34**, 213 (2011).
23. A. Novikov *et al.*, *J. Immunol.* **187**, 2540 (2011).
24. K. D. Mayer-Barber *et al.*, *J. Immunol.* **184**, 3326 (2010).
25. S. Roy *et al.*, *J. Infect. Dis.* **179**, 187 (1999).
26. G. Herrera, *Int. J. Lepr.* **17**, 35 (1949).
27. P. F. Barnes *et al.*, *Infect. Immun.* **61**, 3482 (1993).
28. C. E. Barry 3rd *et al.*, *Nat. Rev. Microbiol.* **7**, 845 (2009).
29. N. R. Gandhi *et al.*, *Lancet* **368**, 1575 (2006).

Acknowledgments: We thank P. Liu for advice with the *M. leprae* viability assays and helpful discussion; M. So for help in the bioinformatic analysis; K. Zavala for help with the high-performance liquid chromatography (HPLC) assays; A. Legaspi and A. DeLeon for help with the immunohistochemistry; M. Schibler and the University of California–Los Angeles, California NanoSystems Institute, Advanced Light Microscopy Core Facility for assistance with the confocal studies; D. Elashoff for help with the statistical analysis; and A. Steinmeyer, E. May, and U. Zügel from Bayer Pharma AG for the VDR antagonist ZK 159 222 (VAZ). The live *M. leprae* was provided by the U.S. National Hansen's Disease Programs through the generous support of the American Leprosy Missions and Society of St. Lazarus of Jerusalem. The data presented in this manuscript are tabulated in the main paper and supplementary materials. Gene expression files containing array data are available under the accession nos. GSE17763 and GSE43700 in the Gene Expression Omnibus (GEO) database. This work was supported in parts by NIH grants (P50 AR063020; R01s AI022553, AR040312, and AI047868; and Clinical and Translational Science Award grant UL1TR000124).

Supplementary Materials

www.sciencemag.org/cgi/content/full/science.1233665/DC1
Materials and Methods
Figs. S1 to S22
References (*30*–*38*)

5 December 2012; accepted 29 January 2013
Published online 28 February 2013;
10.1126/science.1233665

Dual Origin of the Epithelium of the Mammalian Middle Ear

Hannah Thompson and Abigail S. Tucker*

The air-filled cavity and ossicles of the mammalian middle ear conduct sound to the cochlea. Using transgenic mice, we show that the mammalian middle ear develops through cavitation of a neural crest mass. These cells, which previously underwent an epithelial-to-mesenchymal transformation upon leaving the neural tube, undergo a mesenchymal-to-epithelial transformation to form a lining continuous with the endodermally derived auditory tube. The epithelium derived from endodermal cells, which surrounds the auditory tube and eardrum, develops cilia, whereas the neural crest–derived epithelium does not. Thus, the cilia critical to clearing pathogenic infections from the middle ear are distributed according to developmental derivations. A different process of cavitation appears evident in birds and reptiles, indicating that this dual epithelium may be unique to mammals.

The mammalian middle ear is an air-filled cavity housed within the auditory bulla with three ossicles suspended within it, connecting the eardrum to the inner ear. The epithelial lining of the middle ear in the ventral region is continuous with the auditory (Eustachian) tube, which connects the middle ear to the pharynx. At embryonic day 12.5 (E12.5) in the mouse, the ossicles condense within the neural crest–derived first and second pharyngeal arches, adjacent to the developing inner ear and dorsal to the tip of the first pharyngeal pouch (*1*). In early postnatal mice, the future middle ear cavity is filled with neural crest cells surrounding the developing ossicles (*2*), which are positioned in the dorsal region of the future cavity (the attic), in addition to mesodermal cells that will mature to form the middle ear muscles. A process called cavitation then occurs in which the neural crest cells are replaced by an air-filled cavity (*2*, *3*), which surrounds the ossicles and muscles, allowing free movement in response to sound (fig. S1). The whole cavity is lined by an epithelium.

The current model of middle ear cavitation was proposed by Wittmaack (*4*) and suggests that the endoderm of the first pharyngeal pouch extends into the middle ear region, expanding and enveloping the middle ear structures, resulting in a cavity lined completely by endoderm. However, the middle ear cavity has suspended within it three ossicles in addition to muscles, blood vessels, and nerves that would prevent an epithelium expanding through as a continuous sheet. This prompted Schwarzbart to propose that during cavitation the endoderm ruptured and the neural crest formed the lining of the middle ear (*5*). To resolve these issues, we have made use of newly developed transgenic mouse lines *Sox17-2Aicre* (*6*) and *Wnt1cre* (*7*) crossed with the reporter mouse line *R26R* (*8*). When stained with X-Gal, this system permanently labels cells of endodermal or neural crest origin blue and therefore allows the embryonic origin of tissues within the developing middle ear to be determined.

Sox17-2AicreR26R mice trace cells that are currently expressing, or have previously expressed, Sox17. These include cells of endodermal origin and blood vessels. Contrary to previously published data that the epithelial lining of the middle ear is of endodermal origin (*9*, *10*), the fully cavitated middle ear from P14 in *Sox17-2AicreR26R* mice was found to be labeled blue only in the epithelium around the opening to the auditory tube (Fig. 1B), with unstained epithelium around the attic region above the ossicles and along the cochlea (Fig. 1A). To determine the origin of the nonendodermal epithelial cells, *Wnt1creR26R* mice were stained with X-Gal. Around the auditory tube, the epithelium was LacZ-negative (Fig. 1D), whereas the epithelium lining the cavity around the ossicles and cochlea was LacZ-positive (Fig. 1C), in a complementary pattern to that observed in the Sox17-cre line. Careful mapping of the middle ear cavity with these reporter lines showed that the auditory tube and surrounding middle ear epithelium, extending up to and slightly beyond the eardrum on the lateral side, was endoderm-derived. In contrast, neural crest cells were found lining the middle ear cavity on the medial wall covering the otic capsule/cochlea and lining the attic region of the cavity in the vicinity of the ossicles (Fig. 1E) (number of samples analyzed = 15). In humans, the attic is connected to the mastoid air space, and these are therefore also likely to be lined with a neural crest–derived epithelium. The epithelium lining the middle ear cavity is therefore of dual origin, roughly half neural crest and half endodermal.

Department of Craniofacial Development and Stem Cell Biology, King's College London, Guy's Hospital, London, UK, SE1 9RT.
*Corresponding author: abigail.tucker@kcl.ac.uk

If there are neural crest cells lining the middle ear cavity and it is assumed that the middle ear cavity is covered by an epithelium, it suggests that mesenchymal neural crest cells have undergone a mesenchyme-to-epithelium transformation (MET). This would mean that neural crest cells in this region of the ear start life in the neural tube as epithelial, transform to mesenchyme to migrate into the pharyngeal arches, and then transform back to an epithelium. A neural crest origin of the corneal endothelium has previously been shown in the eye (*11*). To confirm whether this was the case in the ear, markers involved in epithelial-mesenchymal transformation (EMT) were investigated. Immunostaining for the epithelial-specific molecule E-cadherin was performed on X-Gal–stained *Wnt1creR26R* postnatal mice. The LacZ-positive blue cells lining the cavity of the middle ear expressed E-cadherin (Fig. 2, A and B). Cytokeratin14 (K14) is an epithelial-specific cytoskeletal protein. Using X-Gal staining on the *K14creR26R* mice (*12*), we observed that the epithelium of neural crest origin at postnatal day 14 (P14) did not express K14 (Fig. 2C); however, by P16 this gene was now expressed by all the epithelium (Fig. 2D). Finally, to determine when the basal lamina of the epithelium was produced, we performed immunostaining against laminin and saw no expression at P14, just as cavitation is completing (Fig. 2E), but strong expression by P19 (Fig. 2F). This suggests that MET of neural crest cells occurs a few days after the cavitation of the ear is complete, resulting in the transformation of the neural crest cells at the retracting edge into an epithelium. A failure in the retraction of this mesenchyme, or a failure in the transformation of the mesenchyme to an epithelium, would result in retention of mesenchyme in the cavity

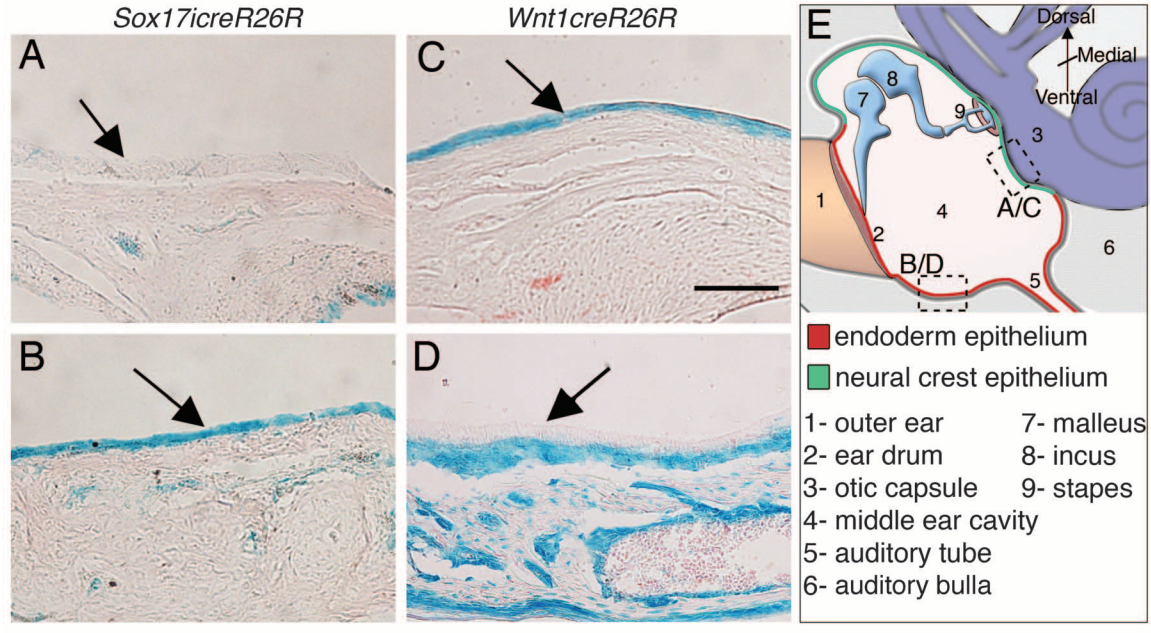

Fig. 1. The epithelial lining of the middle ear cavity is of dual origin. (**A** to **D**) X-Gal and eosin staining of postnatal mouse middle ears. LacZ-negative cells (A) and LacZ-positive cells of endoderm origin (B) are seen lining the middle ear cavity (arrows) in *Sox17-2AicreR26R* at P14. LacZ-positive (C) and LacZ-negative (D) cells are observed (arrows) in *Wnt1creR26R* at P16. (**E**) Schematic representing the distribution of the endoderm and neural crest epithelium and indicating the positions of (A) to (D). Scale bar: 100 μm.

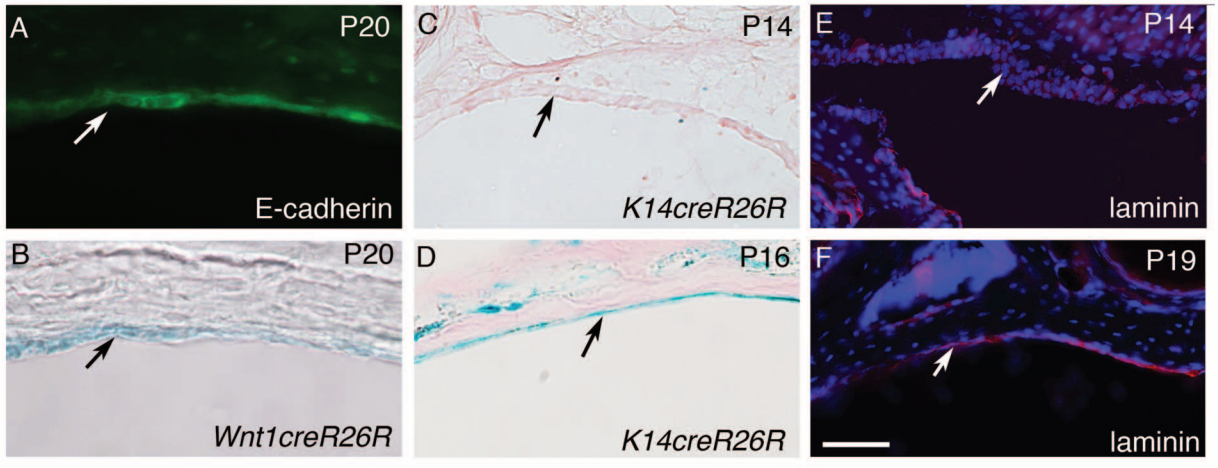

Fig. 2. Neural crest cells in the middle ear undergo a MET. (**A**) P20 *Wnt1creR26R* ear immunostained against E-cadherin (arrow). (**B**) LacZ staining of tissue in (A) shows neural crest origin of E-Cad positive tissue (arrow). (**C** and **D**) X-Gal– and eosin-stained *K14creR26R* neural crest–derived epithelium showing LacZ-negative cells (C) at P14 and Keratin14 expressing blue cells at P16 [arrow in (D)]. (**E** and **F**) Immunostaining against laminin (red) and 4′,6-diamidino-2-phenylindole (DAPI) (blue) showing neural crest epithelium without a basal lamina at P14 [arrow in (E)], but with a basal lamina by P19 [arrow in (F)]. Scale bar: 60 μm.

and air spaces and may explain cases of residual mesenchyme observed in mutant mice and human patients (*3*, *13*).

Previous studies in humans (*14*, *15*), rats (*9*, *16*), and guinea pigs (*17*, *18*) have noted that the epithelium lining the middle ear cavity is of a different type in different regions of the cavity. The middle ear epithelium is known to be either pseudostratified; containing ciliated, goblet, and basal cells; or a simple epithelium without any cilia. We used scanning electron microscopy (SEM) to analyze the distribution of cilia within the mouse middle ear. We found that there were regions of densely ciliated epithelium (Fig. 3A), regions of epithelium with short cilia and long cilia interspersed with a few nonciliated cells (Fig. 3B), and regions of simple epithelium with no cilia (Fig. 3C). The epithelium dense with long cilia was found close to the auditory tube, in the ventral regions of the middle ear, and along the lateral edges of the cavity and was bordered with a region of mixed ciliated and nonciliated cells (Fig. 3D). A number of goblet cells, secreting mucus, were observed restricted to the area entering the auditory tube (Fig. 3A). Over the surface of the otic capsule and lining the attic, the epithelium was nonciliated and simple (Fig. 3D). To compare the epithelial type with embryonic origin, we dissected *Sox17icreR26R* mice in the same way as for SEM and stained with X-Gal to visualize the endoderm-derived epithelium (Fig. 3E). Blue staining was seen in the ventral regions and along the edges of the cavity but not lining the attic in the vicinity of the ossicles or on the medial wall covering the otic capsule. The distribution of ciliated and nonciliated epithelium therefore appears to correspond to the embryonic origin of the cells lining the middle ear cavity. To confirm this, we costained *Wnt1creR26R* middle ears with X-Gal and an antibody against acetylated α-tubulin, which is a marker of cilia. We saw cilia on unstained epithelium of endodermal origin (Fig. 3, F and G) but not on X-Gal–positive epithelium of neural crest origin (Fig. 3, H and I, and fig.S2). In short, the neural crest–derived lining of the middle ear shows several epithelial markers but not the surface cilia typical of mucosal linings.

We have shown that the lining of the middle ear cavity is of both endoderm and neural crest origin and that neural crest cells undergo a mesenchymal-to-epithelial transformation. In this case, the continuity of the endoderm must be breached to allow the neural crest cells to line the upper part of the middle ear cavity. Such a breach has been suggested from histology in the rat (*19*). To find out when and where this takes place, we looked at the embryonic development of the first pharyngeal pouch, as it becomes the future middle ear cavity. At E15.5, the first pharyngeal pouch appears as a continuous epithelium surrounding the future middle ear cavity (Fig. 4A), as shown by the continuous expression of the epithelial cell adhesion molecule E-cadherin (Fig. 4, B and C). By E17.5, the future middle ear cavity appears to be filling with mesenchyme (Fig. 4D) associated with a rupture of the first pharyngeal pouch (Fig. 4, E and F). This shows that during embryonic development in the mouse, the endoderm of the first pharyngeal pouch—after fully extending into the vicinity of the outer and inner ear—breaks down, allowing mesenchyme to fill the future middle ear cavity (Fig. 4G). The middle ear then remains filled with mesenchyme until about P6 (fig. S1A), when the cavitation process begins. Cavitation starts in the ventral region of the middle ear with a retraction of the middle ear mesenchyme away from the endoderm-derived epithelium, producing an air-filled cavity (fig. S1B). This retraction of mesenchyme continues in this way, pulling back past the

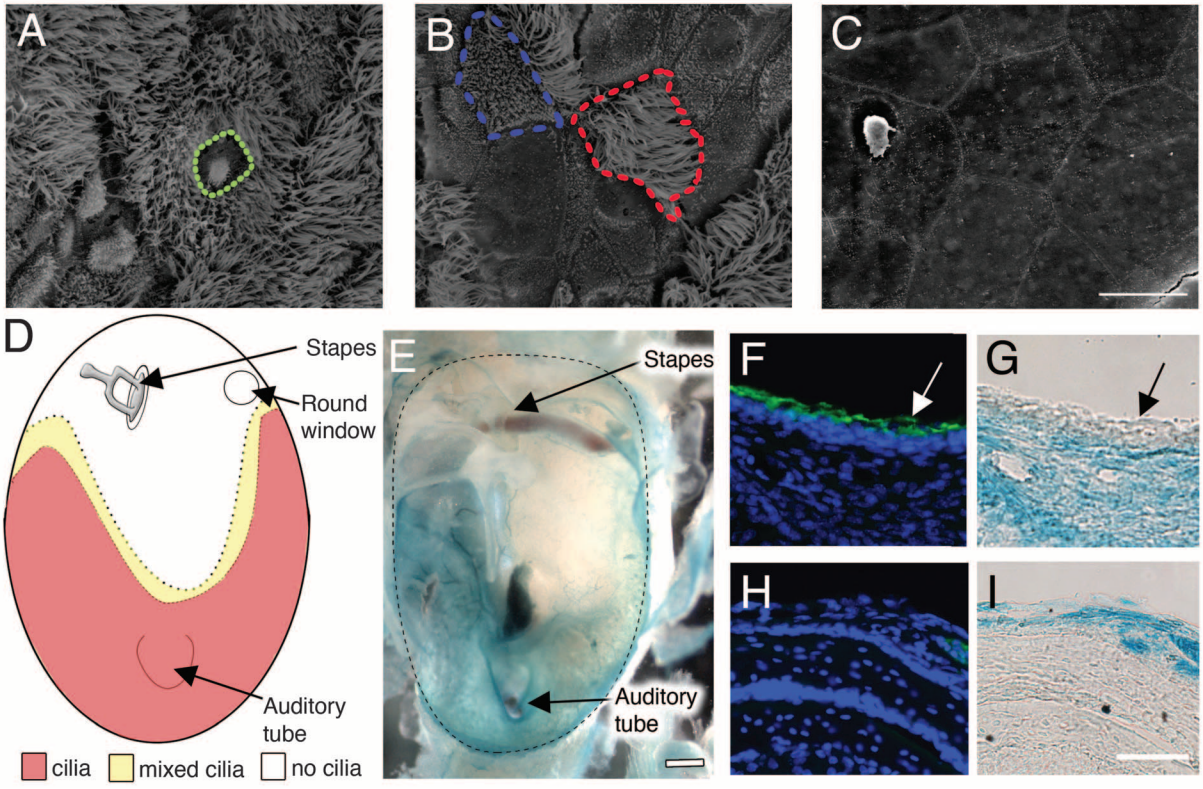

Fig. 3. Middle ear epithelium type is dependent on embryonic origin. (**A** to **C**) SEM imaging of the middle ear cavity surface epithelium, showing regions of densely ciliated cells and a goblet cell (green outline) (A), regions of mixed short-ciliated (blue outline), long-ciliated (red outline), and nonciliated cells (B), and regions of nonciliated epithelium (C). (**D**) Schematic representing the distribution of ciliated epithelium on the middle ear medial wall, with ciliated (red), mixed cilia (yellow), and simple nonciliated (white) regions. (**E**) Whole-mount X-Gal staining of P18 *Sox17-2AicreR26R* middle ear (outlined) dissected by removal of the eardrum revealing the medial wall, showing endoderm (blue) near the auditory tube and along the cavity edges, but not in the center or near the ossicles. (**F** to **I**) *Wnt1creR26R* P12 mice immunostained with acetylated α-tubulin (green), DAPI (blue) [(F) and (H)], and X-Gal stained (blue) [(G) and (I)], showing cilia on *Wnt1creR26R*-negative epithelium [arrows in (F) and (G)], but not on *Wnt1creR26R*-positive epithelium [(H) and (I)]. Scale bars: 10 μm [(A) to (C)]; 500 μm (E); 50 μm [(F) to (I)].

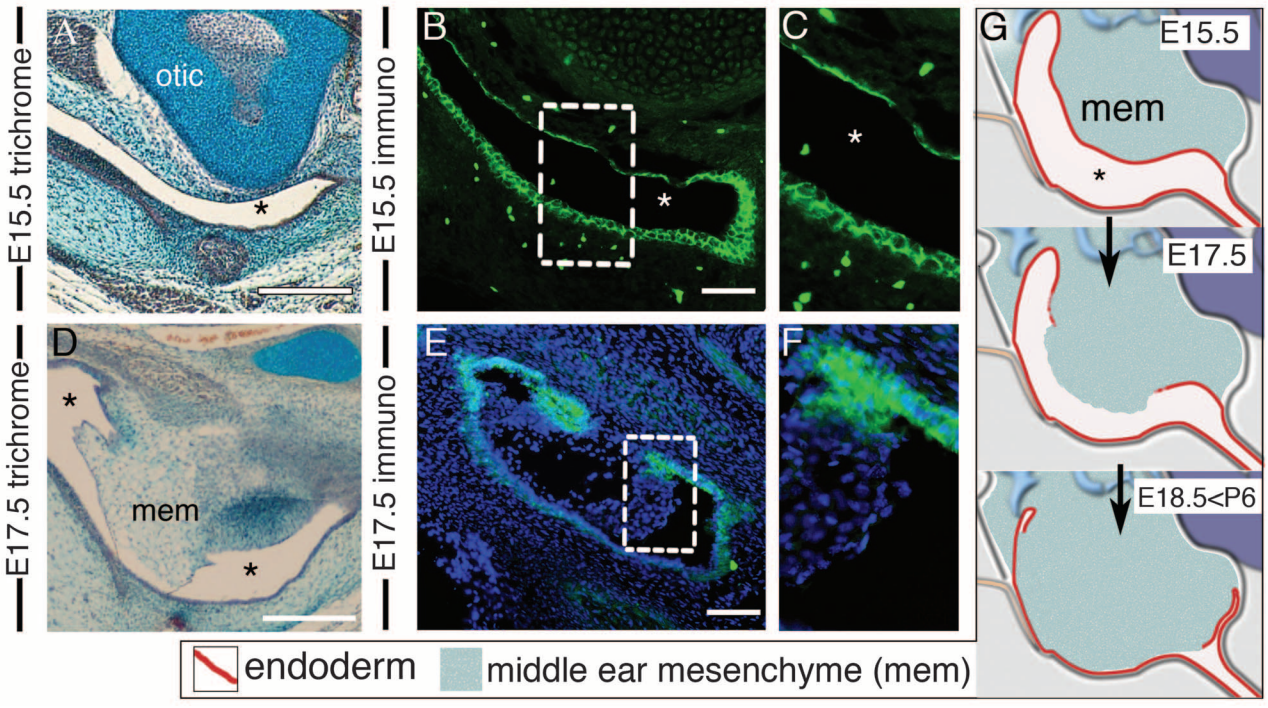

Fig. 4. The first pharyngeal pouch endoderm breaks and mesenchyme fills the middle ear cavity. Embryonic mice with Trichrome staining (**A** and **D**) or immunostained against E-cadherin (**B**, **C**, **E**, and **F**), showing intact epithelium lining the first pharyngeal pouch at E15.5 [(A) to C)] and then broken at E17.5 [(D) to (F)]. (**G**) Schematic representing the endodermal first pharyngeal pouch during embryonic development; from the fully extended pouch with endodermal epithelial lining (red), to breakage of the epithelium, and finally the filling of the middle ear cavity with mesenchyme. Dorsal is top. Otic, otic capsule; *, first pharyngeal pouch cavity. Scale bars: 75 μm [(A) and (D)]; 50 μm [(B) and (E)].

ossicles with the attic clearing last, eventually leaving a completely air-filled cavity (fig. S1C).

The three-ossicle mammalian middle ear is very different from that of other land tetrapods, which possess a single ossicle, the two additional ossicles having evolved by a transformation of the original jaw joint (*20*, *21*). We therefore wanted to assess whether a similar break in the endoderm and influx of mesenchyme into the cavity occurred in nonmammals. In the chick and gecko, no rupture of the endoderm during middle ear development was observed using histology, and mesenchyme did not enter the cavity, which remained air-filled (fig. S3). In contrast, in another mammal, the shrew, a similar filling of the middle ear cavity to that in the mouse was observed during development. Further lineage analysis is necessary to assess whether the middle ear in nonmammals has a dual origin; however, it is interesting to note that a neural crest origin of the middle ear epithelium has not been reported after quail-chick neural crest grafts within this region (*22*, *23*). In addition, unlike the heterogeneous mammalian middle ear epithelium, no regional differences were found in the avian middle ear epithelium, with a fairly simple epithelium being observed in all regions (*24*). It is therefore possible that nonmammals adopt the endodermal model, whereas the mesenchymal model is specific to mammals and may have evolved in connection with the incorporation of the jaw joint into the ear, which required cavitation of a previously solid area of mesenchyme.

We have shown that the highly versatile neural crest cells can undergo a mesenchyme-to-epithelium transformation, but they are unable to form the complex pseudostratified ciliated epithelium associated with the endodermally derived part of the middle ear. This implies that there may be constraints limiting the ability of the neural crest to form advanced epithelial cell types. As the neural crest–derived epithelium is simple and unciliated, its function to clear away mucus and debris efficiently would be limited, compared to the endodermally derived epithelium, which provides a logical explanation for why middle ear infections are more common and more severe in the neural crest–lined attic than in the ventral endoderm–lined region of the cavity (*25*). The origin of the middle ear epithelium therefore may have a direct consequence for health of the mammalian ear.

References and Notes

1. M. H. Kaufmann, *The Atlas of Mouse Development* (Academic Press, London, 1992).
2. K. Park, K. Ueno, D. J. Lim, *Am. J. Otolaryngol.* **13**, 93 (1992).
3. C. A. Richter *et al.*, *Hum. Mol. Genet.* **19**, 1551 (2010).
4. K. Wittmaack, *Uber die Normale und die Pathologische Pneumatisation des Schlaefenbeines* (Gustav Fischer, Jena, Germany, 1918).
5. A. Schwarzbart, *J. Laryngol. Otol.* **73**, 45 (1959).
6. S. Engert, W. P. Liao, I. Burtscher, H. Lickert, *Genesis* **47**, 603 (2009).
7. Y. Chai *et al.*, *Development* **127**, 1671 (2000).
8. P. Soriano, *Nat. Genet.* **21**, 70 (1999).
9. D. A. Hilding, E. Szachowicz, S. A. Larsen, *Am. J. Otolaryngol.* **1**, 97 (1980).
10. B. Proctor, *J. Laryngol. Otol.* **78**, 631 (1964).
11. M. C. Johnston, D. M. Noden, R. D. Hazelton, J. L. Coulombre, A. J. Coulombre, *Exp. Eye Res.* **29**, 27 (1979).
12. A. K. Indra *et al.*, *Horm. Res.* **54**, 296 (2000).
13. V. J. Jaisinghani, M. M. Paparella, P. A. Schachern, D. S. Schneider, C. T. Le, *Am. J. Otolaryngol.* **20**, 363 (1999).
14. J. Sade, *Arch. Otolaryngol.* **84**, 137 (1966).
15. N. H. Buch, M. B. Jorgensen, *Arch. Otolaryngol.* **79**, 472 (1964).
16. W. Kuijpers, J. M. van der Beek, P. H. Jap, E. L. Tonnaer, *Histochem. J.* **16**, 807 (1984).
17. R. Haye, *Cell Tissue Res.* **148**, 431 (1974).
18. D. J. Lim, M. M. Paparella, R. S. Kimura, *Acta Otolaryngol.* **63**, 425 (1967).
19. W. F. Marovitz, E. S. Porubsky, *Ann. Otol. Rhinol. Laryngol.* **80**, 384 (1971).
20. M. Takechi, S. Kuratani, *J. Exp. Zool. B Mol. Dev. Evol.* **314B**, 417 (2010).
21. N. Anthwal, L. Joshi, A. S. Tucker, *J. Anat.* **222**, 147 (2013).
22. G. Köntges, A. Lumsden, *Development* **122**, 3229 (1996).
23. D. M. Noden, *Dev. Biol.* **96**, 144 (1983).
24. F. Giannessi, R. Ruffoli, *J. Anat.* **183**, 103 (1993).
25. S. Varshney *et al.*, *Indian J. Otolaryngol. Head Neck Surg.* **62**, 421 (2010).

Acknowledgments: The authors thank A. Warley and G. Vizcay in the Centre for Ultrastructural Imaging at King's College London for help with the SEM and J. Green for his helpful critique of the manuscript. We also thank H. Lickert and M. A. Basson for the Sox17-2AiCre line. This work was funded by a project grant from the Medical Research Council (G1001232). Sox17-2Aicre transgenic mice are available for noncommercial use subject to a material transfer agreement with Helmholtz Zentrum München, German Research Centre for Environmental Health (GmbH), through H. Lickert.

Supplementary Materials

www.sciencemag.org/cgi/content/full/339/6126/1453/DC1
Materials and Methods
Figs. S1 to S3

16 November 2012; accepted 11 February 2013
10.1126/science.1232862